Research Article

Synthesis of a Novel Ce-bpdc for the Effective Removal of Fluoride from Aqueous Solution

Changqing Zhao,[1] Yanwei Cui,[1] Fang Fang,[1] Si Ok Ryu,[2] and Jiarui Huang[1]

[1]*College of Chemistry and Materials Science, Center for Nano Science and Technology, Anhui Normal University,
 Wuhu, Anhui 241000, China*
[2]*School of Chemical Engineering, Yeungnam University, Gyeongsan, Gyeongbuk 712749, Republic of Korea*

Correspondence should be addressed to Si Ok Ryu; soryu@ynu.ac.kr and Jiarui Huang; jrhuang@mail.ahnu.edu.cn

Ce-1,1′-biphenyl-4,4′-dicarboxylic acid (Ce-bpdc), a novel type of metal organic framework, was synthesized and applied to remove excessive fluoride from water. The structure and morphology of Ce-bpdc were measured by X-ray diffraction, scanning electron microscopy, Fourier transform infrared spectroscopy, and X-ray photoelectron spectroscopy. The effects, such as saturated adsorption capacity, HCO_3^-, and pH, were investigated. The optimal pH value for fluoride adsorption was the range from 5 to 6. The coexisting bicarbonate anions have a little influence on fluoride removal. The fluoride adsorption over the Ce-bpdc adsorbent could reach its equilibrium in about 20 min. The Ce-bpdc coordination complex exhibited high binding capacity for fluoride ions. The maximum adsorption capacity calculated from Langmuir model was high up to 45.5 mg/g at 298 K (pH = 7.0) and the removal efficiency was greater than 80%. In order to investigate the mechanism of fluoride removal, various adsorption isotherms such as Langmuir and Freundlich were fitted. The experimental data revealed that the Langmuir isotherm gave a more satisfactory fit for fluoride removal. Finally, the tested results of ground water samples from three places, Yuefang, Jiangji, and Sanyi which exhibited high removal efficiency, also demonstrate the potential utility of the Ce-bpdc as an effective adsorbent.

1. Introduction

Fluoride ions are ubiquitous in surface and underground water and are one of the critical components for dental and bone health of mammals which are found to be beneficial for the mineralization of hard tissues in the mammal body in a narrow concentration with range of 0.5–1.5 mg/L [1–4], and fluorine and its compounds are valuable and extensively used in industry of fertilizers, high purity graphite, semiconductors, electrolysis of alumina, and so forth [5]. Fluorine ions are found in trace amounts in various tissues of the human body, particularly teeth and bones, where 80%–90% of the fluorine ions in the human body are present. Fluoride ions are also important constituents of bone and teeth; a healthy body requires approximately 1.0 mg of fluorine ions every day. On the other hand, severe side effects, such as bone cancer and fluorosis, can occur when people are exposed to fluoride concentrations in excess of 1.5 mg/L for long periods [6, 7].

Though the presence of fluoride in drinking water is essential for human health, excessive intake of fluoride will result in diseases such as dental, skeletal, or crippling fluorosis in children and fetal cerebral function, neurotransmitters and brain damage, Alzheimer's syndrome, thyroid disorder, and cancer in adults [8–11]. The World Health Organization (WHO) has recommended a guidance value of 1.5 mg/L for fluoride in drinking water, and the permissible concentration of fluoride ions is less than 1.0 mg/L in China [12, 13]. This concern greatly promotes the water community for searching an effective way of defluoridation.

Excess fluoride ions from groundwater for meeting the requirement of drinking water can be removed by various techniques, including ion-exchange [14–16], reverse osmosis [17, 18], dialysis and electrodialysis [19, 20], precipitation [21, 22], membrane separation [23, 24], coagulation sedimentation [25], electrocoagulation [26, 27], and adsorption and biosorption [28–30]. In the previous period, the traditional

method for fluoride removal is to form insoluble salts by adding calcium salt, aluminum salt, or iron salt as precipitant. On the other hand, these classical methods need to add a large amount of precipitate or coprecipitating agent; therefore, these methods are limited because they cannot meet the drinking water standards by the World Health Organization (WHO) [31]. Up to now, several methods are being developed to remove fluoride ions, such as adsorption through the use of metal oxide, metal-loaded synthetic polymer, biopolymer, and some anion exchange resin as efficient defluoridation adsorbents [32, 33]. Although they have already been modernized or studied by some researchers, these methods are still tedious and time-consuming and have no practical applications [34]. Adsorption is a more acceptable defluoridation method and plays an important role in the purification of water with trace levels of fluoride because of the simplicity of design, environmental considerations, effectiveness, and convenience as compared to other methods [31–34]. Adsorbents with favorable structures, high adsorption capacities, and ease of separation are highly desirable. Among the adsorbents used for defluoridation, such as activated carbon [35], metal oxides [36–38], and aluminum based adsorbents [39, 40], aluminum hydroxides receive more attention because of their strong affinity for fluoride and low cost for large-scale production [41]. In recent years, a variety of adsorbents, like Ce(III)-incorporated cross-linked chitosan, Zr(IV) immobilized cross-linked chitosan, and so forth, have been identified for the purpose of defluoridation [9, 42].

Metal organic frameworks (MOFs) constructed by metal-containing nodes connected by organic bridges, as potential adsorbents, attract a great deal of interest because of their large surface areas, adjustable pore sizes, and controllable properties, as well as acceptable thermal stability. MOFs can exhibit ultrahigh porosity and high thermal and chemical stability and have been altered for use in various adsorption-related areas [43]. Recently, a number of researchers started to investigate the capability of MOFs to remove compounds including removal of metal ions [44–46] and toxic dyes [47, 48] in aqueous environment. These studies unveiled the fact that several types of MOFs can remain intact in aqueous solutions and show exceptional capacities to remove pollutants from water compared to traditional adsorbents. Lately, MOFs has also been evaluated for defluoridation in water [23, 49, 50].

More researchers have focused on rare earth metals, and rare earth element hydrous oxides, for example, cerium and lanthanum and its salts, have strong affinity to fluoride, arsenate, and other anions [51]. Cerium is investigated using first-principles calculations based on density functional theory to stabilize the structural and electronic properties [52]. In our present study, Ce-1,1'-biphenyl-4,4'-dicarboxylic acid (Ce-bpdc), a novel type of metal organic framework and novelly defined adsorption for rapid removal of fluoride from aqueous solution, was prepared for the first time. Ce-MOFs adsorbents were prepared and used for fluoride removal, respectively. Ce-MOFs adsorbents were investigated by X-ray diffraction, scanning electron microscopy, Fourier transform infrared spectroscopy, and X-ray photoelectron spectroscopy. The as-prepared adsorbent was also used for treatment of underground water with high fluoride concentration in Yuefang, Jiangji, and Sanyi in Anhui province of China. Thus, it is desirable to develop low cost adsorbents which can efficiently work in a real sample. The maximum adsorption capacity and removal efficiency were studied and had most crucial part in adsorption. This study indicated that Ce-MOFs membrane could be developed into a very viable technology for highly effective removal of fluoride from drinking water.

2. Experimental

2.1. Preparation of Disodium 4,4'-Biphenylenedicarboxylate.
All chemicals used in this study were of pure analytical grade and used without further purification. 5.0 g of 1,1'-biphenyl-4,4'-dicarboxylic acid was dissolved in 80 mL of water in a 250 mL beaker with vigorous stirring, and a uniform cloudy solution was obtained. Subsequently, a 10 M NaOH solution was added dropwise to the above mixed solution with vigorous stirring, until the precipitation disappeared. The mixture solution was then heated and crystallized. The obtained crystals were washed several times with Milli-Q water (18 MΩ) to yield the final product, disodium 4,4'-biphenylenedicarboxylate.

2.2. Preparation of Ce-bpdc Coordination Complex.
Briefly, 3.0 g of disodium 4,4'-biphenylenedicarboxylate was placed into a 100 mL beaker, followed by the addition of an appropriate amount of water for complete dissolution under ultrasonic irradiation. Subsequently, the solution was stirred vigorously with a magnetic agitator. $Ce(NO_3)_3 \cdot 6H_2O$ was dissolved in water and added slowly to the above solution, resulting in a turbid solution, which was stirred for 1 h. The resulting precipitate was centrifuged and washed several times with Milli-Q water and vacuum dried at 50°C for 24 h.

2.3. Characterization.
The products were characterized by X-ray diffraction (XRD, Shimadzu XRD-6000, with high-intensity Cu Kα radiation with a wavelength of 1.54178 Å), scanning electron microscopy (SEM, Hitachi S-4800, operated at 5 kV), and Fourier transform infrared (FT-IR, IRPrestige-21) spectroscopy. X-ray photoelectron spectroscopy (XPS, Thermo ESCALAB 250) was carried out using an Al-Kα 150 W nonmonochromatized X-ray source and a hemispherical energy analyzer at pass energy of 30 eV.

2.4. Detection of Fluoride Ions.
The experiments were performed using the fluoride ion-selective electrode method to detect F$^-$. Because the electromotive force of the primary cell consisted of a fluoride ion-selective electrode and F$^-$ solution and the logarithm of F$^-$ activity had a linear relationship, the electromotive force was measured first, followed by the concentration of the F$^-$ solution. The standard curve method was applied to an analysis of the linear relation: a set of different concentrations of standard F$^-$ solutions were prepared before the concentration of the testing F$^-$ solution was examined. The linear formula could be obtained by checking the electromotive force of the primary cell consisting of an electrode and the standard F$^-$ solution. The concentration
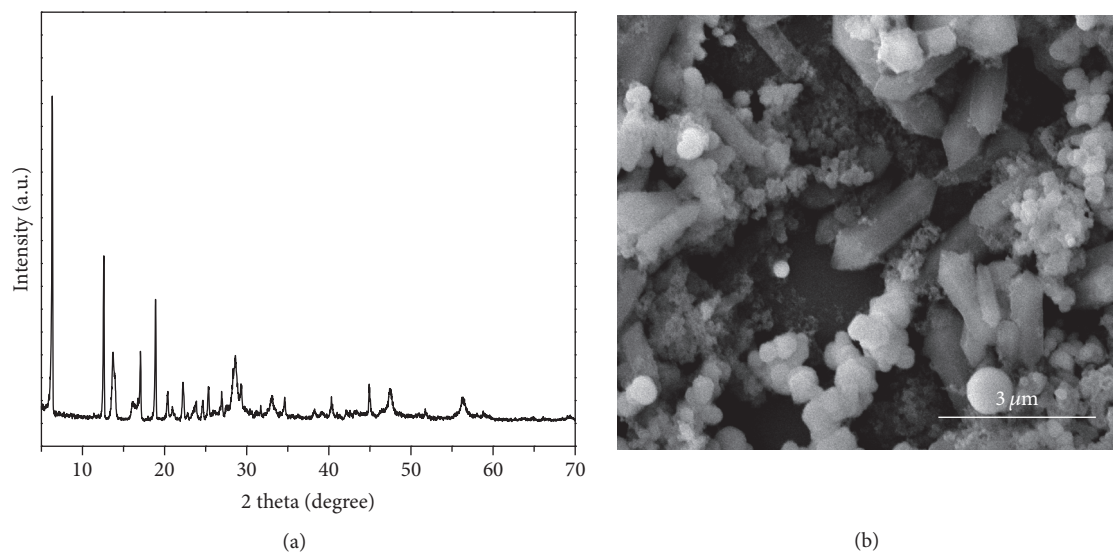
(a)

(b)

FIGURE 1: (a) XRD patterns and (b) SEM image of Ce-bpdc.

of the testing F^- solution can then be obtained using the linear formula and the electromotive force of the primary cell consisted of electrode and the testing F^- solution. The main steps of this method were to immerse the selective electrode into F^- and constitute primary cell and measure the electromotive force of the primary cell using pH meter (model: PHS-3C).

3. Results and Discussion

3.1. Structure and Morphology. The crystal phase of the as-prepared products was characterized by XRD. As shown in Figure 1(a), the XRD peaks of the Ce-bpdc were sharp and intense, indicating the high crystallinity of the Ce-bpdc, and there was a sharp characteristic peak of M-O at approximately 6°. However, it is hard for us to obtain the Ce-bpdc single crystals and the single crystal structure of the new metal organic compound Ce-bpdc cannot be determined by X-ray single crystal structure analysis. Figure 1(b) presents a SEM image of the sample. The as-prepared Ce-bpdc sample had micrometer-sized rod-like and sphere-like shapes.

FT-IR spectroscopy was used to confirm all the functional groups of Ce-bpdc. The FT-IR spectra of the dried Ce-bpdc and diphenyldicarboxylic acid were investigated, as shown in Figure 2. A comparison of the two spectra revealed a red shift in the spectrum of Ce-bpdc, and the characteristic peaks observed at 1584 cm^{-1} and 1528 cm^{-1} were assigned to the COO-Ce. The peak at 3400 cm^{-1} was ascribed to the -OH stretching mode in the coordination complex or H_2O in the sample. The peak at 600–1000 cm^{-1} was assigned to the atomic vibration of benzene ring.

The surface compositions and chemical states of the as-prepared Ce-bpdc were evaluated by XPS. The XPS survey spectrum in Figure 3 indicates the presence of Ce. The peaks at 882.0 eV, 884.0 eV, and 902.0 eV were assigned to Ce^{4+}, $Ce3d_{5/2}$, and $Ce3d_{3/2}$, respectively, which indicates that the
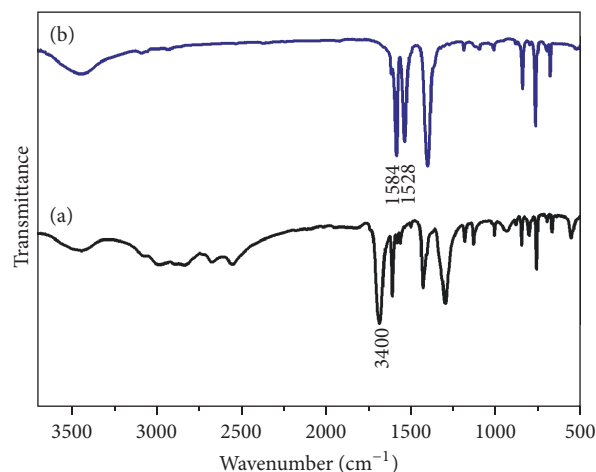

FIGURE 2: FT-IR spectra of (a) bpdc and (b) Ce-bpdc.

valence state of the majority of cerium is +3 and also contains a small amount of Ce^{4+}. In the O1s spectrum, the peaks at 531.9 eV, 532.5 eV, and 532.9 eV were assigned to crystal lattice oxygen, and the peak at 533.9 eV was attributed to adsorbing oxygen in the sample. In the C1s spectrum, the peaks at 285.4 eV, 287.0 eV, and 289.0 eV were ascribed to C-OR, C-X, and MCO_3, respectively, indicating the presence of $CeCO_3$ in Ce-bpdc.

3.2. Adsorption Experiments

3.2.1. Adsorption of pH Dependence. Because OH^- and F^- are isoelectronic species but OH^- is more active than F^-, it can compete with F^- during the adsorption process [53]. As a result, most of the adsorbent material of F^- needs to be used under acidic conditions, which is unavailable for drinking water. Therefore, it is essential to study materials that can
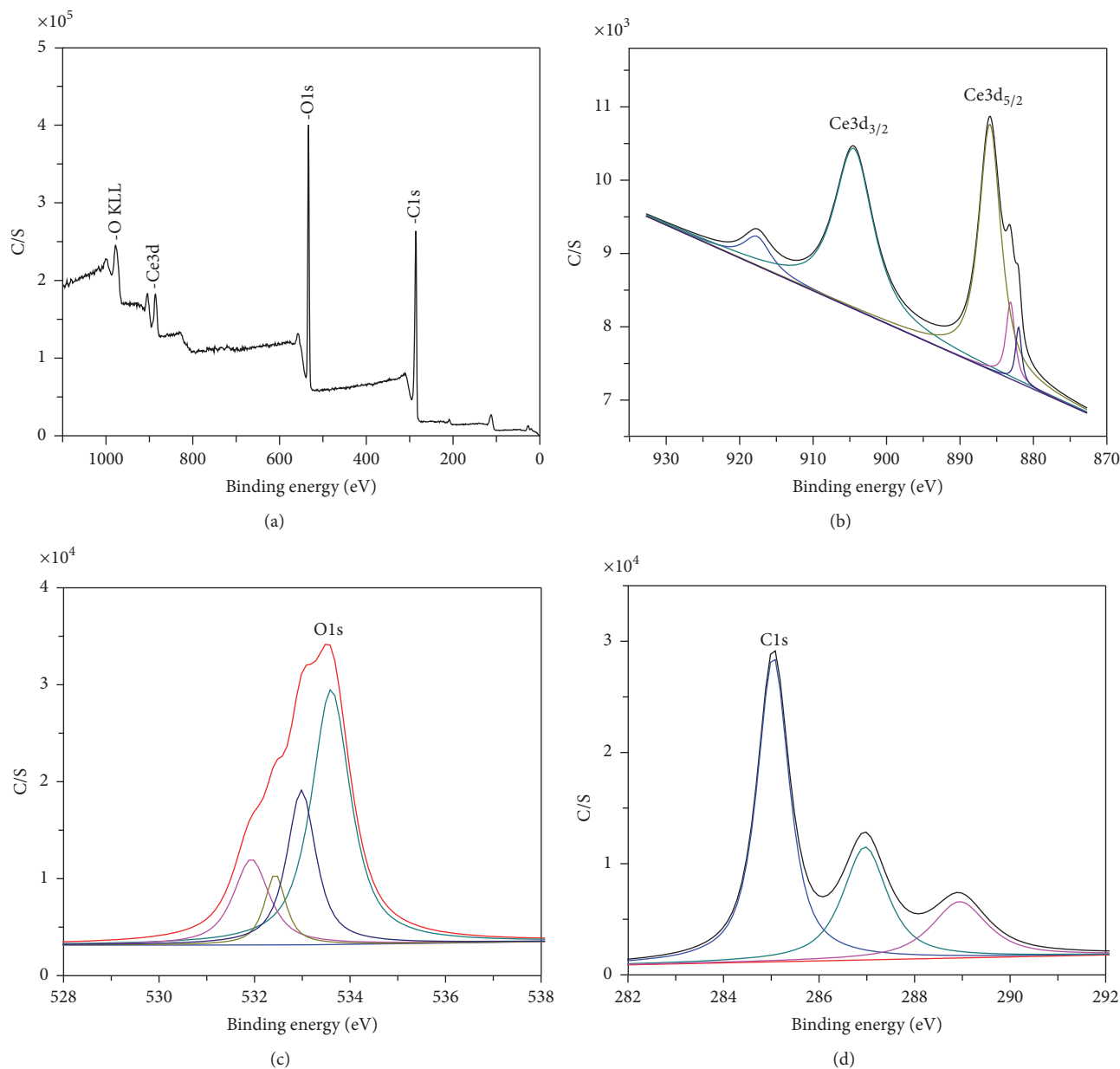
(a)

(b)

(c)

(d)

FIGURE 3: (a) XPS survey spectrum of Ce-bpdc, (b) high-resolution Ce 3d core-level XP spectrum, (c) high-resolution O1s core-level XP spectrum, and (d) high-resolution C1s core-level XP spectrum.

remove F^- under neutral solution conditions. In these experiments, the optimal pH for the removal of F^- by Ce-bpdc was examined; the adsorption experiments were performed at pH = 3.0, 4.0, 5.0, 6.0, 7.0, and 8.0. As shown in Figure 4, when the pH was increased from 3.0 to 5.0, the adsorption capacity increased with increasing pH. On the other hand, the adsorption capacity decreased rapidly when the pH was higher than 6.0. From the above data, Ce-bpdc has the optimal adsorption capacity when the pH is ca. 6.0. Therefore, all the following experiments were conducted at pH = 6.0.

3.2.2. Saturated Adsorption Capacity. The curve of the adsorption capacity of F^- with Ce-bpdc changed with various initial concentrations of solution F^-. As shown in Figure 5, the adsorption capacity increased with increasing F^- concentration. The experimental data was simulated using the Langmuir and Freundlich models, as shown in Figure 5 and Table 1. In Figure 5, the solid line is Langmuir model simulation, and the dashed line is the Freundlich model simulation. From Table 1, the Langmuir model can better represent the data ($R^2 = 0.97515$) than the Freundlich model ($R^2 = 0.81688$), indicating that the adsorption isotherms fit the Langmuir model. Therefore, the adsorption of F^- is due mainly to chemical adsorption with physical adsorption as a complement. The maximum saturation capacity of Ce-bpdc towards F^- is 45.5 mg/g.

TABLE 1: Parameters for the Langmuir and Freundlich models.

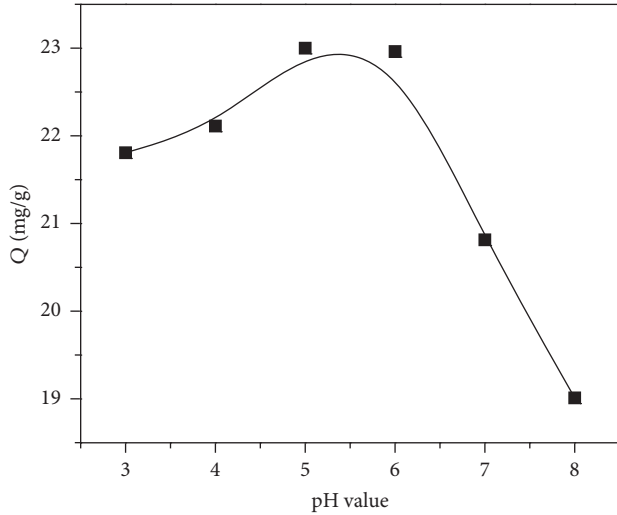|	L-model			F-model	
Q_m	K_L	R^2	n	$\ln K_F$	R^2
45.5 mg/g	0.2265	0.97515	1.818	2.125	0.81688

FIGURE 4: Influence of pH on the adsorption capacity (conditions: adsorption time, 24 h; initial concentration of solution, 24 mg/L; amount of adsorbent, 1.0 g/L).
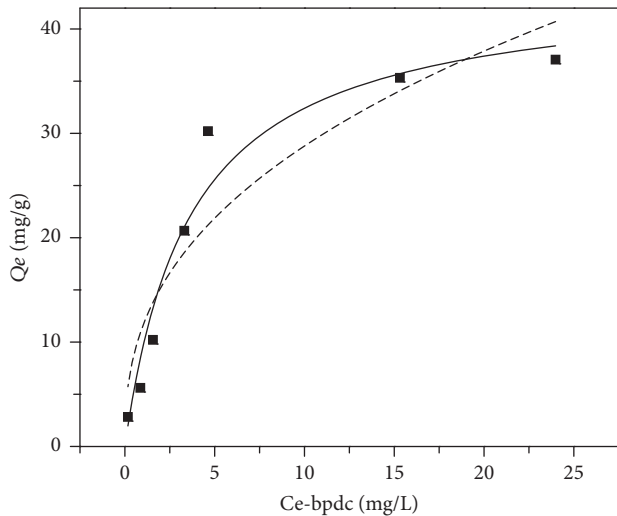

FIGURE 5: Equilibrium adsorption curve (conditions: adsorption time, 24 h; initial concentration of solution, 6–60 mg/L; amount of adsorbent, 1.0 g/L; pH = 5-6). The solid line is Langmuir model simulation, and the dashed line is Freundlich model simulation.

3.2.3. Removal Efficiency.
If an adsorbent has high adsorption capacity, it does not mean that it has high removal efficiency. Therefore, for further analysis of the maximum adsorption capacity, more calculations are needed when the experiments are finished, which can determine if Ce-bpdc can remove fluoride ions from water efficiently. Figure 6 shows that the removal efficiency is greater than 80% when the F^-
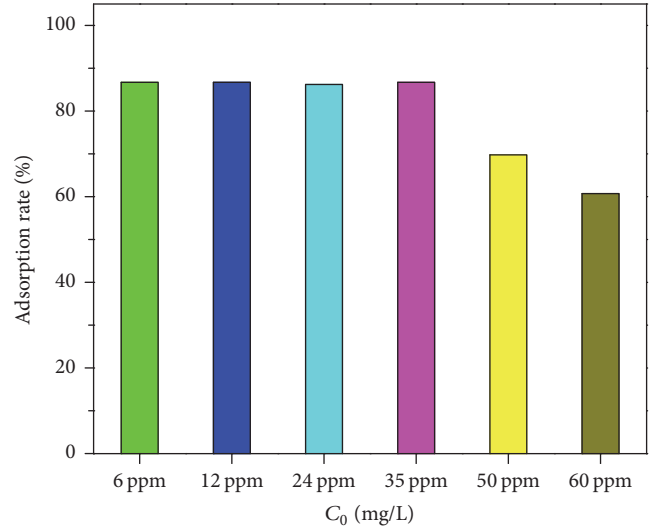

FIGURE 6: Removal efficiency (conditions: adsorption time, 24 h; initial concentration of solution, 6–60 mg/L; amount of adsorbent, 1.0 g/L; pH = 6).

concentration is no more than 35 mg/L. The concentration is below 1 ppm after treatment when the initial concentration of F^- is 6 mg/L. This shows that the Ce-bpdc not only has high adsorption capacity but also has high removal efficiency.

3.2.4. Adsorption Kinetics.
A kinetic study was performed at pH = 6 utilizing a 12 mg/L F^- solution and 1.0 g/L adsorbent in a water bath. 8 mL of the mixed solution was taken out at a certain time. The adsorbent was separated by centrifuge. The concentration of fluoride ions was measured using a fluoride ion-selective electrode. Finally, the adsorption capacities were calculated at different times. Figure 7 shows the adsorption capacities at 2, 5, 10, 15, 20, 30, 60, and 120 min. From Figure 7, the reaction proceeded rapidly in the first 20 min, after which, the reaction reached equilibrium. A pseudo-second-order rate equation was used to simulate the kinetic adsorption as follows:

$$\frac{t}{Q_t} = \frac{1}{2K_2 Q_e^2} + \frac{t}{Q_e}, \tag{1}$$

where K_2 (g/mg·h) is the pseudo-second-order rate constant of adsorption, Q_t (mg/g) is the amount of F^- adsorbed by the adsorbent at time t (min), and Q_e (mg/g) is the equilibrium adsorption capacity. Figure 7 shows a linear plot of t/Q_t versus t. The K_2 value was calculated from the slope and the intercept was 0.067 g/mg·min. The correlation coefficient ($R^2 > 0.999$) for the linear plots is very close to 1, indicating that kinetic adsorption can be described very well using pseudo-second-order kinetics equation.

3.2.5. Effect of HCO_3^-.
In nature, there is a complex chemical environment in water, in which a variety of anions and cations can be found. Among them, the competition among similar type of ions, such as OH^-, HCO_3^-, Cl^-, CO_3^{2-}, and SO_4^{2-}, has a great influence on the removal of contaminant ions by
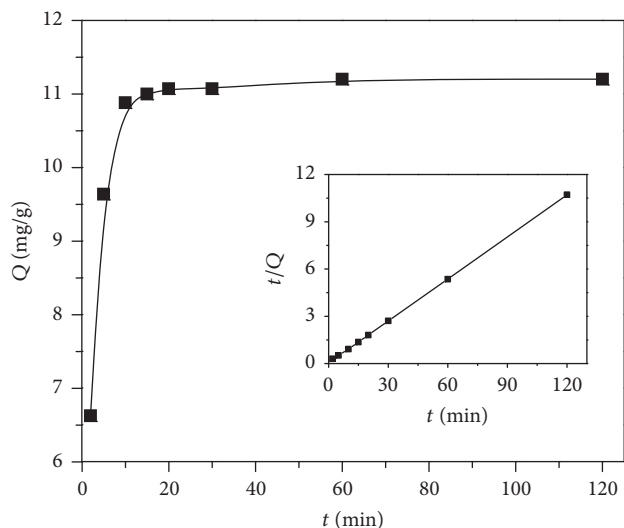
FIGURE 7: Effect of time on the adsorption capacities (conditions: initial concentration of solution, 12 mg/L; amount of adsorbent, 1.0 g/L; pH = 6).

chemical methods. For the removal of fluoride ions, OH^- and HCO_3^- have great influence because OH^- is more active than F^- [54]. Therefore, OH^- has the greatest impact on the removal of F^-. The influence of HCO_3^- has two main aspects: one is the competition with itself and the other is the hydrolysis of HCO_3^-, which can produce OH^- and affect the removal efficiency of F^-. To avoid the effects of OH^-, the pH of the solution was adjusted to 6.0. In this study, the effects of HCO_3^- on the adsorption efficiency were also investigated. By adding 1.0 g/L of adsorbent to 3.0 mg/L of initial concentration of F^- solution, the pH of the solution was adjusted to 6.0, and the solution was shaken for 24 h. The final results are shown in Figure 8. The removal efficiency was 84% when there was no HCO_3^- in the solution. On the other hand, the removal efficiency decreased sharply to 40% when there was 50 mg/L HCO_3^- in solution. The removal efficiency decreased with increasing HCO_3^- concentration.

3.2.6. Study of Real Water Samples. The real water samples from Yuefang, Jiangji, and Sanyi were used to check the application of the product. First, the pH of the real water samples was adjusted to 6.0, and 1 g/L of Ce-bpdc was then added. Table 2 lists all the experimental data; the initial concentrations of F^- in the real water samples from Yuefang, Jiangji, and Sanyi were 3.69, 3.69, and 3.83 mg/L, respectively. After the reaction with Ce-bpdc for 24 h, the concentration of F^- in the real water samples from Yuefang, Jiangji, and Sanyi decreased to 0.86, 1.29, and 1.88 mg/L, respectively, giving corresponding removal efficiencies of 78%, 64%, and 50%. Therefore, Ce-bpdc has high practical value in the removal of fluoride ions from real water samples.

4. Conclusions

Ce-bpdc, a novel type of metal organic framework, was synthesized by a facile simple chemical method. This study

TABLE 2: Treatment of real water samples by Ce-bpdc.

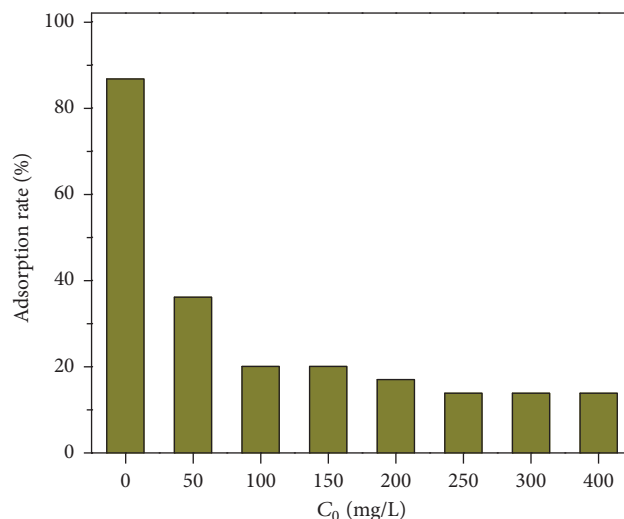| Places	Before treatment (mg/L)	After treatment (mg/L)
Yuefang	3.69	0.86
Jiangji	3.69	1.29
Sanyi	3.83	1.88

FIGURE 8: Effect of HCO_3^- on the adsorption efficiency (conditions: adsorption time, 24 h; initial concentration of F^-, 3 mg/L; amount of adsorbent, 1.0 g/L; pH = 6).

investigated these factors affecting fluoride adsorption onto Ce-bpdc, including coexisting bicarbonate anions, pH value of fluoride solution, and contact time. The Langmuir isotherm mode fitted the equilibrium data well, and the maximum adsorption capacity was up to 45.5 mg/g for fluoride at 298 K and natural pH (6.0), and the removal efficiency was greater than 80%. The adsorption of F^- was mainly due to chemical adsorption with physical adsorption as a complement. The tested results of ground water samples from three places, Yuefang, Jiangji, and Sanyi which exhibited high removal efficiency, indicated that the Ce-bpdc could be effectively employed as a promising defluoridating agent.

Conflicts of Interest

The authors declare that they have no conflicts of interest.

Authors' Contributions

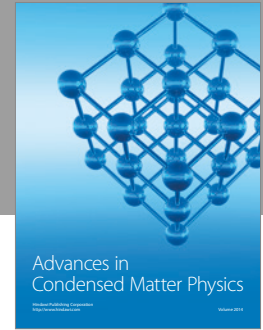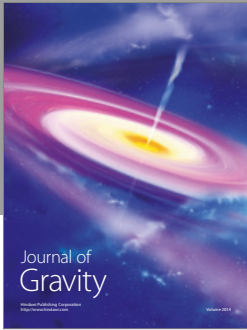Changqing Zhao and Yanwei Cui equally contributed to this work as co-first authors.

Acknowledgments

References

[1] P. Miretzky and A. Fernandez-Cirelli, "Fluoride removal from water by chitosan derivatives and composites: a review," *Journal of Fluorine Chemistry*, vol. 132, no. 4, pp. 231–240, 2011.

[2] S. Dong and Y. Wang, "Characterization and adsorption properties of a lanthanum-loaded magnetic cationic hydrogel composite for fluoride removal," *Water Research*, vol. 88, pp. 852–860, 2016.

[3] B.-S. Zhu, Y. Jia, Z. Jin et al., "Controlled synthesis of natroalunite microtubes and spheres with excellent fluoride removal performance," *Chemical Engineering Journal*, vol. 271, pp. 240–251, 2015.

[4] S. Wu, K. Zhang, J. He et al., "High efficient removal of fluoride from aqueous solution by a novel hydroxyl aluminum oxalate adsorbent," *Journal of Colloid and Interface Science*, vol. 464, pp. 238–245, 2016.

[5] X. Zhao, P. Zhang, Y. Wang, J. Xiong, and B. Tao, "Decomposition and oriented growth of $YBa_2Cu_3O_{7-x}$ films prepared with low fluorine TFA-MOD approach," *Advances in Condensed Matter Physics*, vol. 2013, Article ID 532181, 5 pages, 2013.

[6] B. Kebede, A. Beyene, F. Fufa, M. Megersa, and M. Behm, "Experimental evaluation of sorptive removal of fluoride from drinking water using iron ore," *Applied Water Science*, vol. 6, no. 1, pp. 57–65, 2016.

[7] W. Tang, P. Kovalsky, D. He, and T. D. Waite, "Fluoride and nitrate removal from brackish groundwaters by batch-mode capacitive deionization," *Water Research*, vol. 84, pp. 342–349, 2015.

[8] P. S. Ghosal and A. K. Gupta, "Enhanced efficiency of ANN using non-linear regression for modeling adsorptive removal of fluoride by calcined Ca-Al-(NO_3)-LDH," *Journal of Molecular Liquids*, vol. 222, pp. 564–570, 2016.

[9] Q. Liu, L. Zhang, B. Yang, and R. Huang, "Removal of fluoride from aqueous solution using Zr(IV) immobilized cross-linked chitosan," *International Journal of Biological Macromolecules*, vol. 77, pp. 15–23, 2015.

[10] A. Bhatnagar, E. Kumar, and M. Sillanpää, "Fluoride removal from water by adsorption—a review," *Chemical Engineering Journal*, vol. 171, no. 3, pp. 811–840, 2011.

[11] Y. Fan, D. Fu, S. Zhou et al., "Facile synthesis of goethite anchored regenerated graphene oxide nanocomposite and its application in the removal of fluoride from drinking water," *Desalination and Water Treatment*, vol. 57, no. 58, pp. 28393–28404, 2016.

[12] S. V. Jadhav, E. Bringas, G. D. Yadav, V. K. Rathod, I. Ortiz, and K. V. Marathe, "Arsenic and fluoride contaminated groundwaters: a review of current technologies for contaminants removal," *Journal of Environmental Management*, vol. 162, pp. 306–325, 2015.

[13] A. Fakhri, "Application of response surface methodology to optimize the process variables for fluoride ion removal using maghemite nanoparticles," *Journal of Saudi Chemical Society*, vol. 18, no. 4, pp. 340–347, 2014.

[14] S. Meenakshi and N. Viswanathan, "Identification of selective ion-exchange resin for fluoride sorption," *Journal of Colloid and Interface Science*, vol. 308, no. 2, pp. 438–450, 2007.

[15] K. Vaaramaa and J. Lehto, "Removal of metals and anions from drinking water by ion exchange," *Desalination*, vol. 155, no. 2, pp. 157–170, 2003.

[16] L. Gómez-Hortigüela, A. B. Pinar, J. Pérez-Pariente, T. Sani, Y. Chebude, and I. Díaz, "Ion-exchange in natural zeolite stilbite and significance in defluoridation ability," *Microporous and Mesoporous Materials*, vol. 193, pp. 93–102, 2014.

[17] I. Bejaoui, A. Mnif, and B. Hamrouni, "Performance of reverse osmosis and nanofiltration in the removal of fluoride from model water and metal packaging industrial effluent," *Separation Science and Technology*, vol. 49, no. 8, pp. 1135–1145, 2014.

[18] J. Shen and A. Schäfer, "Removal of fluoride and uranium by nanofiltration and reverse osmosis: a review," *Chemosphere*, vol. 117, no. 1, pp. 679–691, 2014.

[19] M. B. S. Ali, B. Hamrouni, and M. Dhahbi, "Electrodialytic defluoridation of brackish water: effect of process parameters and water characteristics," *Clean - Soil, Air, Water*, vol. 38, no. 7, pp. 623–629, 2010.

[20] P. Sehn, "Fluoride removal with extra low energy reverse osmosis membranes: three years of large scale field experience in Finland," *Desalination*, vol. 223, no. 1-3, pp. 73–84, 2008.

[21] H. M. Huang, J. H. Liu, P. Zhang, D. D. Zhang, and F. M. Gao, "Investigation on the simultaneous removal of fluoride, ammonia nitrogen and phosphate from semiconductor wastewater using chemical precipitation," *Chemical Engineering Journal*, vol. 307, pp. 696–706, 2017.

[22] A. Dhillon, S. Prasad, and D. Kumar, "Recent advances and spectroscopic perspectives in fluoride removal," *Applied Spectroscopy Reviews*, vol. 52, no. 3, pp. 175–230, 2016.

[23] J. He, X. Cai, K. Chen et al., "Performance of a novelly-defined zirconium metal-organic frameworks adsorption membrane in fluoride removal," *Journal of Colloid and Interface Science*, vol. 484, pp. 162–172, 2016.

[24] A. Boubakri, R. Bouchrit, A. Hafiane, and S. Al-Tahar Bouguecha, "Fluoride removal from aqueous solution by direct contact membrane distillation: theoretical and experimental studies," *Environmental Science and Pollution Research*, vol. 21, no. 17, pp. 10493–10501, 2014.

[25] Y. Xue, K. Yang, and J. Mei, "Study of influence factor of fluorine removal from fluorinated water using coagulating sedimentation method," *Engineering Journal of Wuhan University*, vol. 43, pp. 477–493, 2010.

[26] H. Z. Zhao, B. Zhao, W. Yang, and T. H. Li, "Effects of Ca^{2+} and Mg^{2+} on defluoration in the electrocoagulation process," *Environmental Science and Technology*, vol. 44, no. 23, pp. 9112–9116, 2010.

[27] R. Sinha, S. Mathur, and U. Brighu, "Aluminium removal from water after defluoridation with the electrocoagulation process," *Environmental Technology*, vol. 36, no. 21, pp. 2724–2731, 2015.

[28] E. W. Wambu, W. O. Ambusso, C. Onindo, and G. K. Muthakia, "Review of fluoride removal from water by adsorption using soil adsorbents – an evaluation of the status," *Journal of Water Reuse and Desalination*, vol. 6, no. 1, pp. 1–29, 2016.

[29] Y. Duan, C. C. Wang, X. D. Li, and W. Xu, "Fluoride adsorption properties of three modified forms of activated alumina in drinking water," *Journal of Water & Health*, vol. 12, no. 4, pp. 715–721, 2014.

[30] A. Goswami and M. K. Purkait, "Kinetic and equilibrium study for the fluoride adsorption using pyrophyllite," *Separation Science and Technology*, vol. 46, no. 11, pp. 1797–1807, 2011.

[31] S. S. Tripathy, J.-L. Bersillon, and K. Gopal, "Removal of fluoride from drinking water by adsorption onto alum-impregnated activated alumina," *Separation and Purification Technology*, vol. 50, no. 3, pp. 310–317, 2006.

[32] E. Vences-Alvarez, L. H. Velazquez-Jimenez, L. F. Chazaro-Ruiz, P. E. Diaz-Flores, and J. R. Rangel-Mendez, "Fluoride removal

in water by a hybrid adsorbent lanthanum-carbon," *Journal of Colloid and Interface Science*, vol. 455, pp. 194–202, 2015.

[33] H. Paudyal, B. Pangeni, K. Inoue et al., "Adsorptive removal of fluoride from aqueous solution using orange waste loaded with multi-valent metal ions," *Journal of Hazardous Materials*, vol. 192, no. 2, pp. 676–682, 2011.

[34] M. Mouelhi, I. Marzouk, and B. Hamrouni, "Optimization studies for water defluoridation by adsorption: application of a design of experiments," *Desalination and Water Treatment*, vol. 57, no. 21, pp. 9889–9899, 2016.

[35] N. A. Salem and S. M. Ebrahim Yakoot, "Adsorption kinetic and mechanism studies of thorium on nitric acid oxidized activated carbon," *Desalination and Water Treatment*, vol. 57, no. 58, pp. 28313–28322, 2016.

[36] L.-X. Li, D. Xu, X.-Q. Li, W.-C. Liu, and Y. Jia, "Excellent fluoride removal properties of porous hollow MgO microspheres," *New Journal of Chemistry*, vol. 38, no. 11, pp. 5445–5452, 2014.

[37] K. Parashar, N. Ballav, S. Debnath, K. Pillay, and A. Maity, "Rapid and efficient removal of fluoride ions from aqueous solution using a polypyrrole coated hydrous tin oxide nanocomposite," *Journal of Colloid and Interface Science*, vol. 476, pp. 103–118, 2016.

[38] Z. Jin, Y. Jia, K.-S. Zhang et al., "Effective removal of fluoride by porous MgO nanoplates and its adsorption mechanism," *Journal of Alloys and Compounds*, vol. 675, pp. 292–300, 2016.

[39] R. Sun, H.-B. Zhang, J. Qu, H. Yao, J. Yao, and Z.-Z. Yu, "Super-critical carbon dioxide fluid assisted synthesis of hierarchical AlOOH@reduced graphene oxide hybrids for efficient removal of fluoride ions," *Chemical Engineering Journal*, vol. 292, pp. 174–182, 2016.

[40] G. Demirkalp, S. Alamut, O. Arara, U. Yuksel, and M. Yuksel, "Removal of fluoride from water by Al(III)-loaded and Al(OH)$_3$-coated chelating resin," *Desalination and Water Treatment*, vol. 57, no. 11, pp. 15910–15919, 2015.

[41] C. Yang, J. Xiong, J. Wei, J. Wu, B. Zhang, and X. Luo, "High performance enhancement-mode AlGaN/GaN MIS-HEMT with selective fluorine treatment," *Advances in Condensed Matter Physics*, vol. 2015, Article ID 267680, 7 pages, 2015.

[42] J. Li, Q. Liu, R. Huang, and G. Wang, "Synthesis of a novel Ce(III)-incorporated cross-linked chitosan and its effective removal of fluoride from aqueous solution," *Journal of Rare Earths*, vol. 34, no. 10, pp. 1053–1061, 2016.

[43] T. Hang, W. Zhang, H.-Y. Ye, and R.-G. Xiong, "Metal-organic complex ferroelectrics," *Chemical Society Reviews*, vol. 40, no. 7, pp. 3577–3598, 2011.

[44] S. Naeimi and H. Faghihian, "Performance of novel adsorbent prepared by magnetic metal-organic framework (MOF) modified by potassium nickel hexacyanoferrate for removal of Cs$^+$ from aqueous solution," *Separation and Purification Technology*, vol. 175, pp. 255–265, 2017.

[45] Y. Y. Xiong, J. Q. Li, L. L. Gong et al., "Using MOF-74 for Hg^{2+} removal from ultra-low concentration aqueous solution," *Journal of Solid State Chemistry*, vol. 246, pp. 16–22, 2017.

[46] F. Ke, L.-G. Qiu, Y.-P. Yuan et al., "Thiol-functionalization of metal-organic framework by a facile coordination-based postsynthetic strategy and enhanced removal of Hg^{2+} from water," *Journal of Hazardous Materials*, vol. 196, pp. 36–43, 2011.

[47] C. Li, Z. Xiong, J. Zhang, and C. Wu, "The strengthening role of the amino group in metal-organic framework MIL-53 (Al) for methylene blue and malachite green dye adsorption," *Journal of Chemical and Engineering Data*, vol. 60, no. 11, pp. 3414–3422, 2015.

[48] L. Li, J. C. Li, Z. Rao, G. W. Song, and B. Hu, "Metal organic framework [Cu$_3$(BTC)$_2$(H$_2$O)$_3$] for the adsorption of methylene blue from aqueous solution," *Desalination and Water Treatment*, vol. 52, no. 37–39, pp. 7332–7338, 2014.

[49] K.-Y. A. Lin, Y.-T. Liu, and S.-Y. Chen, "Adsorption of fluoride to UiO-66-NH$_2$ in water: stability, kinetic, isotherm and thermodynamic studies," *Journal of Colloid and Interface Science*, vol. 461, no. 37–39, pp. 79–87, 2016.

[50] F. Ke, G. Luo, P. Chen et al., "Porous metal-organic frameworks adsorbents as a potential platform for defluoridation of water," *Journal of Porous Materials*, vol. 23, no. 4, pp. 1065–1073, 2016.

[51] S. Zhang, Y. Lü, X. Lin, Y. Zhang, and X. Su, "Performance and mechanisms of fluoride removal from groundwater by lanthanum-aluminum-loaded hydrothermal palygorskite composite," *Chemical Research in Chinese Universities*, vol. 31, no. 1, pp. 144–148, 2015.

[52] Y. Guo, T. Jia, C. Li, Y. Niu, S. Hou, and S. Liu, "Theoretical investigation on structural and electronic properties of InN growth on Ce-stabilized zirconia (111) substrates," *Advances in Condensed Matter Physics*, vol. 2016, Article ID 9435387, 7 pages, 2016.

[53] S. Hokkanen, A. Bhatnagar, and M. Sillanpää, "A review on modification methods to cellulose-based adsorbents to improve adsorption capacity," *Water Research*, vol. 91, pp. 156–173, 2016.

[54] Y.-X. Zhang and Y. Jia, "Preparation of porous alumina hollow spheres as an adsorbent for fluoride removal from water with low aluminum residual," *Ceramics International*, vol. 42, no. 15, pp. 17472–17481, 2016.

Journal of
Gravity

Journal of
Photonics

The Scientific
World Journal

Journal of
Soft Matter

Advances in
Condensed Matter Physics

Journal of
Fluids

Journal of
Aerodynamics

International Journal of
Statistical Mechanics

International Journal of
Optics

Hindawi

Submit your manuscripts at
https://www.hindawi.com

Journal of
Computational
Methods in Physics

Advances in
High Energy Physics

Journal of
Thermodynamics

Physics
Research International

Advances in
Astronomy

Journal of
Solid State Physics

Journal of
Astrophysics

International Journal of
Superconductivity

Journal of
Biophysics

Journal of
Atomic and
Molecular Physics